Time-Resolved Laser-Induced Fluorescence Measurements in the Plume of a 6-kW Hall Thruster

IEPC-2015-399／ISTS-2015-b-399

Presented at Joint Conference of 30th International Symposium on Space Technology and Science 34th International Electric Propulsion Conference and 6th Nano-satellite Symposium, Hyogo-Kobe, Japan July 4 – 10, 2015

Christopher J. Durot,[1] Marcel P. Georgin,[2] and Alec D. Gallimore[3]
University of Michigan, Ann Arbor, Michigan, 48105, USA

Abstract: **A new technique to measure oscillations in the ion velocity distribution is applied for the first time to a Hall thruster. To our knowledge, these are the first measurements of time-resolved laser-induced fluorescence on unperturbed Hall thruster operating conditions at a variety of magnetic field settings. We present an initial dataset showing that ion dynamics clearly change depending on the magnetic field setting at the 150 V, 10 mg/s operating condition. At the nominal magnetic field, the mean velocity of the distribution oscillates approximately periodically, while the metastable ion density oscillates out of phase with mean velocity. At lower magnetic field, a more intense oscillation occurs with a wider range of mean velocity and metastable ion density, which periodically disappears below the noise floor. Higher than nominal magnetic field stabilizes ion dynamics with a smaller range of mean velocity and an approximately constant metastable ion density, though the oscillations are not approximately periodic. We also examine the evolution of the ion VDF between the discharge channel and plume at the nominal field. The width of the distribution at the downstream point is periodically explained by velocity bunching at certain times but not others, implying that there are some other processes intermittently widening the distribution. Finally, benchmarking to help confirm accurate results from the new technique is also discussed.**

Nomenclature

B_r	=	radial magnetic field magnitude at a given magnetic circuit current setting
B_r^*	=	radial magnetic field magnitude at the nominal magnetic circuit current
c	=	speed of light in vacuum
Δf	=	Doppler frequency shift in the ion frame
f_0	=	laser frequency in the lab frame
$FWHM_{meas}$	=	measured full width at half max at z = 15 mm as a function of time
$FWHM_{theory}$	=	full width at half max at z = 15 mm as a function of time predicted from kinematic compression
I_{IM}	=	inner magnet current setting
$\hat{k}$	=	unit wave vector of the laser
m	=	spoke mode number, the number of complete periods in the discharge channel circumference
$\vec{v}$	=	ion velocity vector
v	=	ion axial speed
z	=	axial location of the interrogation zone relative to the thruster exit plant

[1] Ph.D. Candidate, Applied Physics, durot@umich.edu
[2] Ph.D. Precandidate, Applied Physics, georginm@umich.edu
[3] Arthur F. Thurnau Professor, Aerospace Engineering, alec.gallimore@umich.edu

I. Introduction

We present an initial campaign using transfer function laser-induced fluorescence (TFLIF) with the H6 Hall thruster. TFLIF is a technique, recently developed and validated[1], to measure the time-resolved ion velocity distribution function (VDF) using laser-induced fluorescence (LIF). The goal of this paper is to demonstrate some of the capabilities of the TFLIF system developed at the Plasmadynamics and Electric Propulsion Laboratory (PEPL). We investigate two phenomena: (1) how the ion velocity distribution changes with the thruster operating mode during a magnetic field sweep, and (2) how the ion VDF evolves between points upstream and downstream of the exit plane.

A discharge voltage of 150 V and a flow rate of 10 mg/s were used to maximize the LIF signal-to-noise ratio (SNR). The SNR was much lower at discharge voltages of 150 V and 300 V than previously reported with the H6 at this facility[2]. The cause is currently unknown but will be investigated to allow measurement at the nominal 300 V condition.

Table 1 summarizes the different conditions interrogated. Many more spatial locations and a more complete magnetic field sweep were planned, but the loss of laser alignment due to facility problems consumed much of the time allotted for this campaign. The plan was consequently pared down to the smallest set of point that could still yield interesting results. The data presented here were all taken in two days near the end of March 2015.

Table 1. Test matrix of conditions where TFLIF signal was captured during this campaign. All data taken at the H6 150 V, 10 mg/s operating condition along the channel centerline at 3 O'clock. Green cells denote data was taken and presented. Analysis failed to yield reasonable results for data taken at the exit plane with nominal field (red cell) for unknown reasons.

		Z (mm)		
		- 4	0	15
B_r/B_r^*	0.5238		green	
	1	green	red	green
	1.48		green	

A number of other supporting measurements were made with the LIF from the photomultiplier. High-speed discharge current and floating probe measurements (5 mean discharge channel diameters downstream) provide two different input signals for either transfer function averaging or to define triggers for triggered averaging. Luminous intensity in the thruster channel was measured with the FASTCAM to further correlate and validate TFLIF results.

II. Background

A. Oscillations and Mode Transitions in the H6

Brown found transitions between two distinct operating modes on the H6 Hall thruster[3] in a study of operation at low discharge voltages of 100-120 V and anode mass flow rates of 10 - 20 mg/s. The thruster transitioned from a "low-current" mode to an undesirable "high-current" mode as discharge voltage was reduced. A lower cathode flow fraction reduced stability such that a transition to a high-current mode occurred at a higher voltage, but auxiliary neutral flow outside of the cathode could stave off the transition.

The two modes were called "low-current" and "high-current" modes due to an approximately 10% difference in mean discharge current. The other key features that Brown found to distinguish high-current mode from low-mode are a lower thrust-to-power ratio and current utilization (ratio of ion beam current to discharge current), larger beam divergence, and larger amplitude discharge current oscillations by about a factor of ten. A hysteresis effect enabled operation in both modes at some operating conditions. Though the amplitude of oscillations changed in different modes, the peak frequencies were the same in both modes at the same operating condition. Brown observed a sudden change in the plume at the transition, shown in Figure 1. The luminous plume in high-current mode extends further downstream, has a more prominent

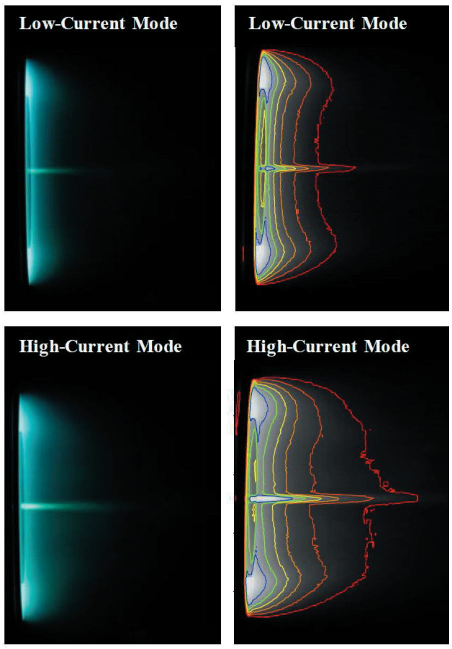

Figure 1. Photos of the H6 plume (left) and contours of constant intensity (right) for both low-current mode (upper) and high-current mode (lower). Reproduced from Brown[3].

central spike, and is generally brighter.

Using an E×B probe and a retarding potential analyzer, measurements of the ion energy and ion energy per charge distributions in the far field plume were well defined in low-current mode but highly diffuse in high-current mode, possibly even showing bimodal distributions. Though the ion distributions clearly differed between the two modes, gaining quantitative information about ion distributions was difficult since the exact contributions from different ionization states were unknown.

LIF would help uncover more information about the ion distributions in the two modes because it can be spatially resolved and the ion velocity distribution is measured directly without confounding multiple charge states. Time-resolved LIF would even enable measurements of oscillations in the distribution, possibly explaining the bimodal form and elucidating any differences in the ion dynamics of the two modes.

Sekerak conducted a study[4] of thruster modes as a function of magnetic field magnitude at discharge voltage of 300-450 V and anode mass flow rate of 14.7-25.2 mg/s. Sekerak found two modes with the same general features as the modes observed by Brown at low voltage conditions. The higher current mode (by about 15% in mean discharge current) was again found to be related to ten times higher amplitude discharge current oscillations (almost 100% of the mean value) and a 25% lower thrust-to-power ratio. Figure 2 shows the trends in discharge current and oscillation amplitude during magnetic field sweeps. Changes in light emission in the plume were very similar to those observed by brown. The higher current mode has generally brighter emission, a more prominent central spike, and more emission that occurs further downstream. In contrast with Brown's findings, the thruster was more sensitive to a transition to a high-current mode for higher discharge voltage and higher anode flow rate operating conditions.

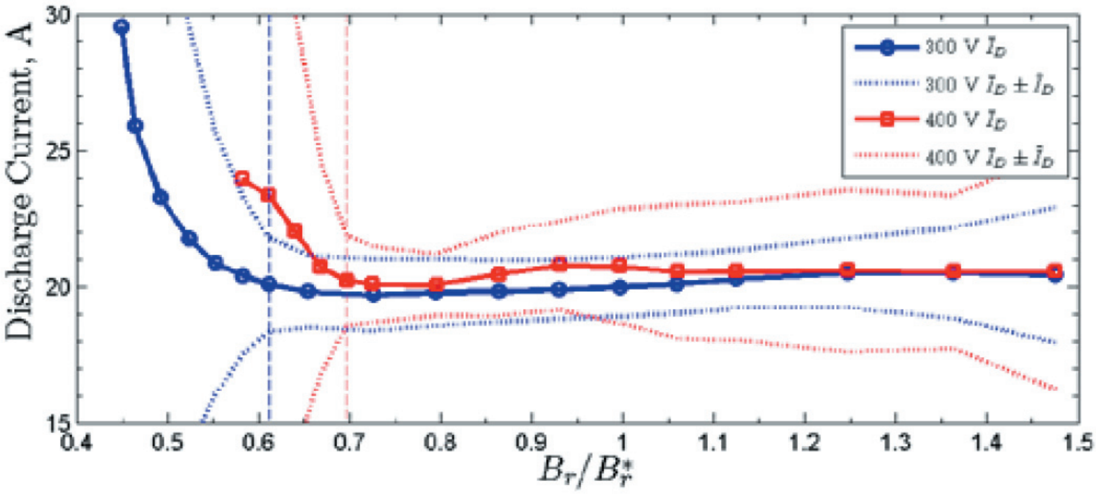

Figure 2. Mean discharge current (solid lines) and RMS oscillation amplitude (dotted lines) as a function of magnetic field magnitude at discharge voltages of 300 V (blue) and 400 V (red). Reproduced from Sekerak[4].

Sekerak also conducted an extensive test of oscillations as the thruster transitioned between the two modes using a high-speed camera and Langmuir probes. In general, the higher-current mode was found to be associated with a global oscillation in phase at all azimuthal locations, and the lower-current mode was associated with localized, azimuthally propagating spokes, which lead to the terms "global mode" for the higher-current mode and "local mode" for the lower-current mode. The local mode is associated with the best thruster performance in terms of thrust-to-power since it minimizes discharge current.

Sekerak used a method similar to that developed by McDonald to describe spokes in terms of power spectral density and mode number[5]. The spoke mode number m corresponds to the number of oscillation periods across the circumference of the discharge channel. That is, m = 1 corresponds to a perturbation of a single spoke traveling azimuthally, m = 2 corresponds to two spokes, and so on. The global mode, with no spokes and a uniform oscillation throughout the channel is referred to as the m = 0 mode. The thruster can exhibit several modes of azimuthal spokes mixed together, and is frequently more chaotic than global mode oscillations.

B. Laser-Induced Fluorescence Background

Laser-induced fluorescence can be used to measure the velocity distribution of a specific species of ions or neutral atoms. It takes advantage of the Doppler shift of the laser wavelength needed to excite a transition to induce fluorescence. For a nonrelativistic speed v opposing the laser, the laser frequency will be shifted in the frame of the ion by:

$$\frac{\Delta f}{f_0} = -\frac{\vec{v} \cdot \hat{k}}{c} = \frac{v}{c}, \tag{1}$$

where Δf is the frequency shift observed by ions at speed v, f_0 is the laser frequency in the lab frame, c is the speed of light, and $\hat{k}$ is the unit wave vector. LIF of xenon ions in Hall thrusters typically uses a three level system. Metastable ions are probed at 834.724 nm (wavelength in air), and fluorescence is collected at 541.9 nm. A transition to the higher energy state can occur when the shifted laser frequency observed by the ions equals the atomic line frequency. Once excited, the ions fluoresce in a time on the order of nanoseconds. The collected fluorescence is proportional to the density of ions within the interrogation volume in the metastable state and moving at speed v. To measure the velocity distribution, the laser frequency is scanned over a range near the transition to collect the relative density of ions moving at all relevant velocities.

The background light collected from the plasma can be orders of magnitude more intense than the LIF, making measurements challenging. LIF studies using a CW laser often use a lock-in amplifier to recover the LIF signal from the background light emitted by the discharge. The raw signal-to-noise ratio (SNR) of this signal is typically so poor that the lock-in amplifier must be set to an integration time constant of at least 100 ms, destroying time resolution. Hence, LIF measurements in plasma have traditionally been time-averaged. Many new techniques have been developed in recent years to measure time-resolved LIF (TRLIF) signals plasma sources such as Hall thrusters. Most examples recover the signal from the noise by form of averaging in the time domain triggered off of the phase of an oscillation of the plasma source, but all other TRLIF techniques implicitly assume periodic oscillations in the averaging process.

For example, one TRLIF approach for a pulsed plasma source uses a lock-in amplifier with a short integration time constant and an oscilloscope set to average over many time-series triggered at the beginning of a pulse[6,7,8]. This technique allows a trade-off between SNR improvement from the lock-in amplifier and time resolution, while the remaining necessary SNR improvement comes from averaging over many pulses.

MacDonald, Cappelli, and Hargus developed a TRLIF system that uses a sample-and-hold circuit to hold the signal level at a given phase of the oscillation and send that signal into a lock-in amplifier to recover the signal from the noise[9]. Since the signal into the lock-in amplifier is held at a certain phase of the oscillation, time-resolved signal recovery is made possible using a low-frequency laser modulation of 11 Hz and a typical commercial lock-in amplifier.

Mazouffre et al. implemented a TRLIF approach using a discriminator and multichannel scaler to average time-series of photon counts collected over many oscillation periods. This system averages out noise by using a low-frequency laser modulation (20 Hz), adding counts collected when the laser is on (signal plus noise), and subtracting counts collected when the laser is off (noise only)[10,11]. When applied to a Hall thruster, the need for relatively periodic oscillations and repeatable triggering was overcome by periodically cutting off the thruster discharge current for a short time and triggering each time-series by the cutoff. The plasma at reignition resulted in quasi-periodic oscillations that behaved much like natural breathing mode oscillations, but the ion VDF was changed by the perturbation in discharge current[12]. A perturbation to the cathode keeper potential was found to create relatively periodic oscillations amenable to the averaging technique without significantly changing the average ion VDF[13].

A heterodyne technique developed by Raitses et al. does not involve a triggered average, but it does require periodic oscillations[14]. For a Hall thruster, this requirement necessitates driving more periodic oscillations (the anode potential was driven at the natural breathing mode peak frequency). The key assumption of the heterodyne technique is that the ion velocity distribution oscillation will be some arbitrary function that is periodically repeating with the same frequency as the discharge oscillation, in which case the signal can be decomposed into a Fourier series that includes components only from the driving frequency and its harmonics. The heterodyne technique involves injecting the laser at some modulation frequency and then using a normal lock-in amplifier to recover the heterodyne signal at a frequency of $n\omega_D \pm \omega_L$, where ω_D is the driving frequency, ω_L is the laser modulation frequency, and n is the order of the component collected.

III. Experimental Configuration

The TRLIF technique developed at PEPL works with the analog photomultiplier signal and high speed laser modulation (on the order of megahertz) well above low frequency Hall thruster oscillations. This allows the use of band-pass filtering and phase-sensitive detection as signal conditioning to demodulate the signal and raise SNR before digitization and averaging over many oscillation cycles. In order to avoid the need for triggering and an assumption of periodic oscillations, and therefore to avoid the need to perturb natural thruster operation, we use a method of averaging empirically estimated transfer functions that was first used at PEPL for high-speed Langmuir probes[15]. Hence the PEPL TRLIF technique is called transfer function laser-induced fluorescence (TFLIF). The key assumption is that the thruster acts as a time invariant linear system with some transfer function mapping the input signal (such as discharge current or floating probe voltage) to the LIF signal as the system output. Due to the time invariance, the transfer function itself is assumed constant while the thruster operates at single operating condition in equilibrium, but the individual oscillations that go into calculating the ensemble of empirically estimated transfer functions need not be periodic or repeatable. Once a high SNR average transfer function is obtained, it can be used with any input signal to calculate the characteristic output signal (the TRLIF signal) associated with that input. The details of the optics, electronics, and signal processing technique were described in a recent journal paper[1]. That paper also included validation with a hollow cathode plasma source and periodic discharge oscillations.

A diagram of the experimental setup inside the Large Vacuum Test Facility is shown in Figure 3. The laser, propagating along the thruster axis to measure axial velocity, is focused to a 1 mm spot near the thruster exit plane. A 75-mm-diameter lens with 85-mm focal length images light collected from the interrogation volume onto a 1-mm optical fiber with unity magnification. Light is collected 30 degrees from the exit plane, defining a small interrogation volume about 1 mm in all dimensions. All points interrogated are along the discharge channel centerline at the thruster's 3 O'clock position. The laser is radially polarized to excite primarily π transitions in the thruster's radial magnetic field, reducing Zeeman splitting [16].

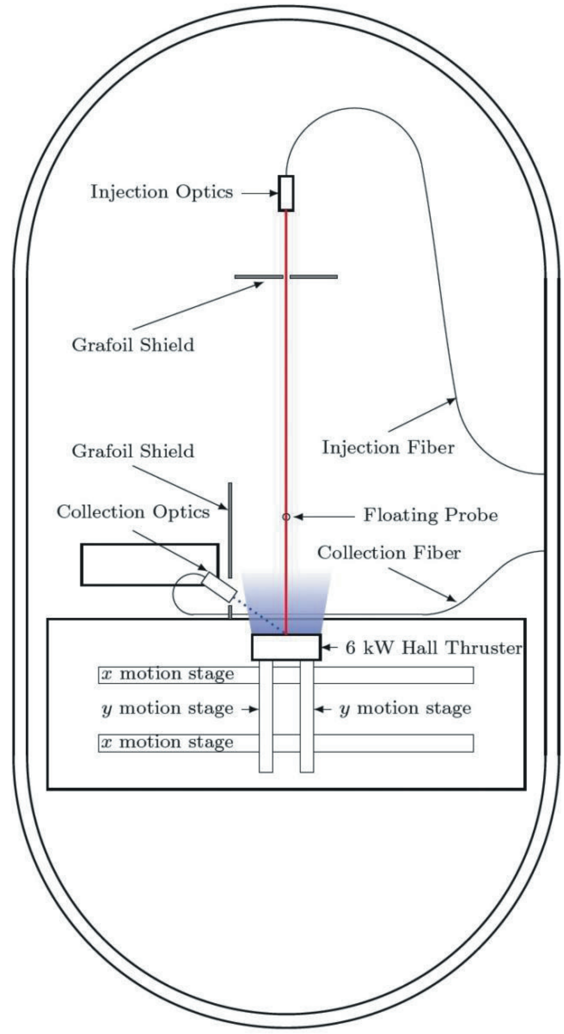

Figure 3. Diagram of the experimental setup inside the Large Vacuum Test Facility.

Both optics and their structures are protected from ion bombardment behind graphite shields and glass windows. A floating probe is placed five thruster diameters downstream along the 6 O'clock channel centerline for use as a transfer function input alternative to the discharge current, though no measurements making use of the probe are reported in this paper. The thruster itself is mounted on x-y motion stages to move the stationary interrogation volume relative to the thruster.

High-speed video of the thruster nearly head-on was captured in this campaign to compare with TRLIF data. The high-speed image analysis technique is described in detail by McDonald[5] and Sekerak[4], but we outline here the basic idea of the analysis and the parameters used for this campaign. The camera captures a resolution of 256x256 at a frame rate of 87500 Hz for a total of 2^{14} frames, or about 0.19 s. The oscillation is AC coupled by subtracting the mean image from each frame. The discharge channel annulus is divided into 180 azimuthal bins of 2 degree extent. The average intensity of all pixels in each bin is taken to be the bin intensity, giving a 180 x 16384 vector representing intensity in cylindrical coordinates for each frame in time. A 2D discrete Fourier transform leads to the power spectral density for each spoke mode. High-speed video was triggered simultaneously with the digitizer measuring PMT voltage, discharge current, and floating probe potential.

IV. Results

A. Comparing Upstream and Downstream Velocity Distributions

Time-resolved ion VDFs were measured at two locations at nominal magnetic field (inner magnet current 3.5 A). These points demonstrate data collection in both the relatively hot and dense plasma in the discharge channel and the cooler and rarer plasma in the plume. The point in the discharge is 4 mm upstream of the exit plane (z = -4 mm), and the point in the plume is 15 mm downstream (z = 15 mm). The points were chosen based on electron density and temperature maps at 300 V from Reid[17]. Density and temperature were not mapped at 150 V, but maps of electric field at 150 V in Appendix C show that the plasma properties likely have a similar spatial trend.

The measured ion velocity distribution at z = -4 mm is shown in Figure 4. There is an approximately periodic oscillation with a high density population of ions forming at a minimum in mean velocity near 3.5 km/s. The mean velocity then increases to a maximum of about 5 km/s. After reaching the maximum velocity, the population density and distribution spread suddenly fall and the mean velocity declines back to the minimum at approximately the same rate as the rise in velocity. The oscillation then begins again, leading to a shape similar to a triangle wave. There is a long low energy tail extending almost to 0 m/s that only appears when the bulk velocity is near its minimum.

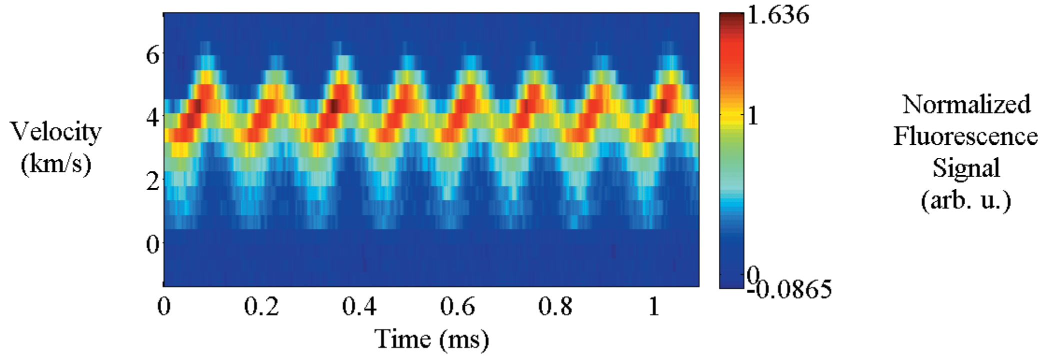

Figure 4. Ion velocity distribution as a function of time at z = -4 mm for the 150V, 10 mg/s operating condition of the H6.

The measured ion velocity distribution at z = 15 mm is shown in Figure 5. The LIF signal was much weaker at this point, which is apparent in the lower signal-to-noise ratio, though the maximum in the time-averaged signal is normalized to 1. The basic features are similar to the z = - 4 mm point. A similar oscillation in mean velocity occurs between about 10 and 12 km/s at z = 15 mm. Density similarly falls as the mean velocity begins to decline, but the rate of decline increases slightly toward the minimum in mean velocity, leaving a small kink in the downward part of the plot. The maximum in bulk distribution spread occurs at the minimum of mean velocity. The low velocity tail is less pronounced at this location and is largely obscured by the noise.

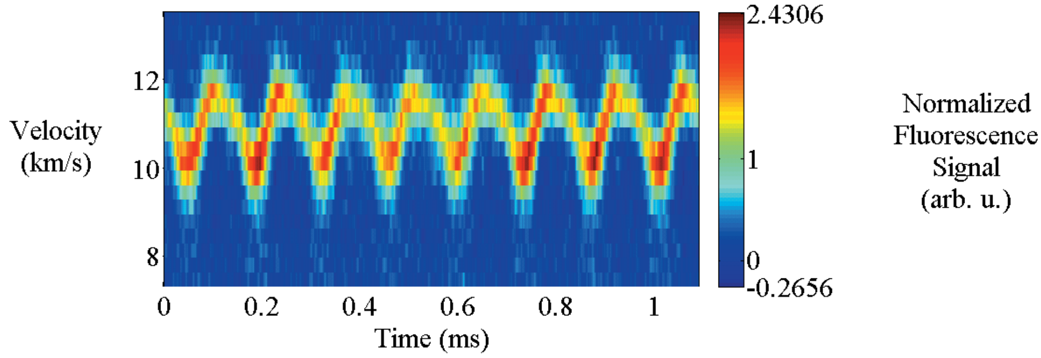

Figure 5. Ion velocity distribution as a function of time at z = 15 mm for the 150 V, 10 mg/s operating condition of the H6.

The distribution is significantly narrower downstream. The change in the distribution spread can be partially explained by kinematic compression or velocity bunching, an effect whereby a velocity spread narrows due to an acceleration[18,19]. Intuitively, it occurs because fast ions spend less time in the accelerating potential than slow ions, and therefore receive a smaller increment in velocity, hence the velocity spread between them is reduced. Bunching can make a prediction of the distribution FWHM at z = 15 mm based on the FWHM at z = -4 mm and the potential drop observed between z = - 4 mm and z = 15 mm. For simplicity, we assume that the distribution at z = 15 mm will only depend on the accelerated ions from the z = - 4 mm distribution at the same time. In reality, the ions at z = 15 mm at a certain time will have come from z = - 4 mm at slightly different times (and some even may have been born downstream of z = - 4 mm), but the simplifying assumption is reasonable since even slow ions with an average speed of 3 km/s will travel the 19 mm distance in about 6 μs, a time in which the VDF changes little and that is near the time resolution of this data set.

The ratio of the measured width ($FWHM_{meas}$) to the predicted width ($FWHM_{theory}$), plotted in Figure 6, oscillates between about 1 (about the same as predicted) and 3 (3 times as wide as predicted). The plot is very noisy due to the uncertainty in measuring FWHM in both distributions and the potential drop between the two points, but the oscillation in the ratio of $FWHM_{meas}$ to $FWHM_{theory}$ is strongly correlated with but slightly out of phase with the discharge current oscillation. This behavior may be evidence of an ionization zone oscillating in axial position. When the ratio is greater than 1, there may be significant ionization downstream of z = - 4 mm, leading to a wider distribution than predicted by bunching alone calculated from the distribution at z = - 4 mm. When the ratio is near 1, there may be little ionization downstream of z = - 4 mm, and therefore distribution spread at z = 15 mm downstream is well explained by bunching. The possibility of an oscillation in the position of the ionization zone is a hypothesis for which evidence has been observed in Hall thrusters (e.g. Mazouffre[10,11]), but a more complete data set is needed to confirm it in the H6.

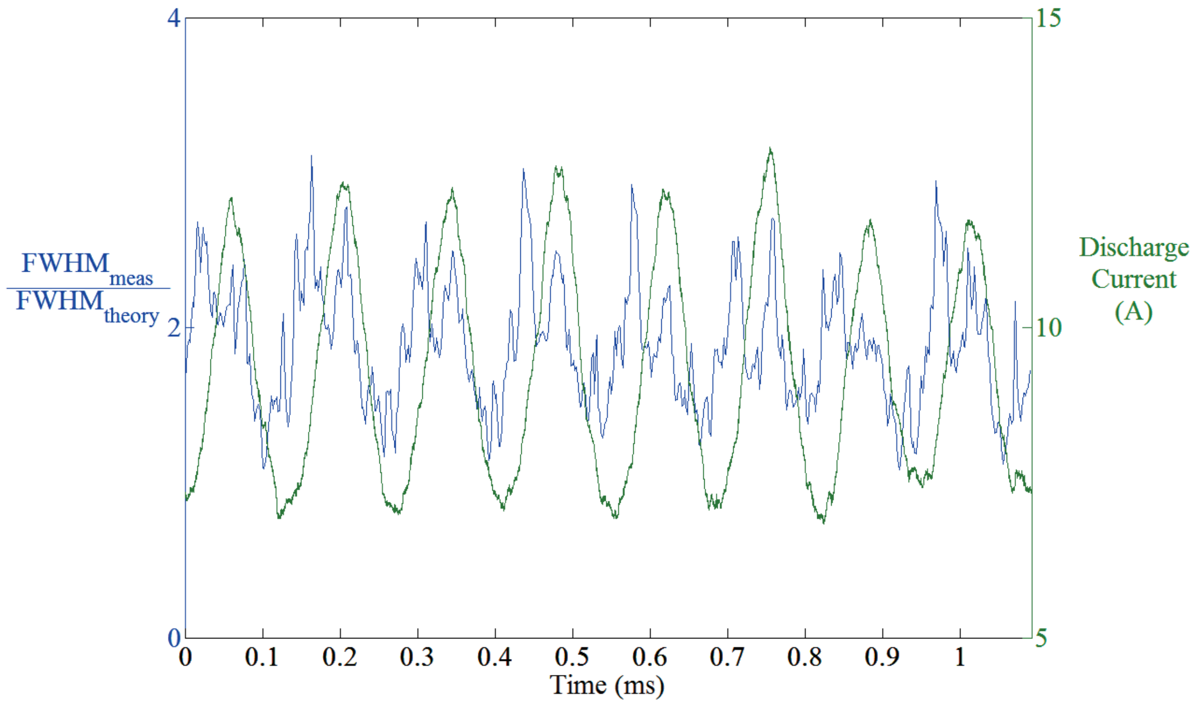

Figure 6. Ratio of measured ion velocity distribution FWHM at z = 15 mm to that predicted by bunching given the ion velocity distribution at z = -4 mm. It oscillates between approximately 1 and 3, highly correlated with discharge current oscillations, and possibly indicates axial motion of the ionization zone.

B. The Effect of Varying Magnetic Field

The thruster's magnetic field was varied to observe changes such as the thruster operating mode transitions observed with the H6 by Sekerak[4]. This reference also briefly presents a least squares fit to predict magnetic field magnitude from Infolytica MagNet simulations. The magnetic field magnitude, normalized by the nominal magnetic field magnitude B_r^*, is given as a function of inner magnet current in amperes I_{IM} by:

$$B_r / B_r^* = -0.0105 I_{IM}^2 + 0.3343 I_{IM} - 0.0444 \, . \tag{2}$$

This formula assumes a constant ratio of inner magnet current to outer magnet current of 1.12 to ensure a constant field shape while varying only field magnitude. This ratio was maintained throughout this campaign. A sweep of magnetic field to map out thruster operating modes at many field magnitudes was planned but time allowed for only three magnetic field points to be measured.

A Photron SA5 FASTCAM capturing luminous intensity in the discharge channel helped assess the thruster operating mode and mode transitions by detecting the global and local oscillations briefly described in the introduction. High-speed camera footage was captured simultaneously with some of the TRLIF data with a resolution of 256x256 and a frame rate of 87500 Hz. This FASTCAM data was then processed by a version of the analysis originally developed by McDonald to quantify the presence of spokes and global oscillations[5].

Figure 7 presents the power spectral density of the FASTCAM intensity at the three magnetic field settings tested. The low field condition has by far the strongest global mode oscillation with sharp peaks and four harmonics visible up to the Nyquist frequency. The spoke modes have peaks at the same frequencies as the global mode, an effect also observed[4] at the same low field magnitude and discharge voltage of 300 V and anode flow rate of 19.5 mg/s. The global mode dominated and there were no visible azimuthal perturbations in the high-speed video, thus the relatively strong m > 1 peaks are likely smearing from the m = 0 peaks, as described by McDonald[5]. Turbulent azimuthal perturbations were visually present at the nominal field but the (weaker) global oscillation continued to dominate. The high field condition had the weakest and broadest global mode peak. The spoke mode peaks had mostly vanished, but the power spectral density of the noise floor is higher than at the other field magnitudes. The strongest azimuthal perturbations were observed at this condition, but they were highly random and not coherent spokes due to the spectra similar to white noise. In general, the peaks tend to decrease in frequency with increasing magnetic field, also in agreement with Sekerak's results.

$\boldsymbol{B_r/B_r^* = 0.52}$ $\boldsymbol{B_r/B_r^* = 1}$ $\boldsymbol{B_r/B_r^* = 1.48}$

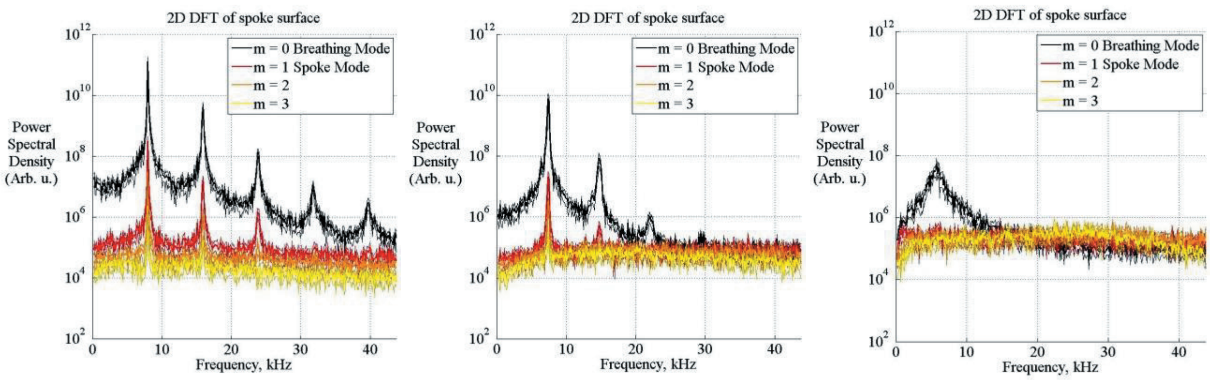

Figure 7. Power spectral density of FASTCAM intensity for the m = 0 breathing mode and spoke modes m = 1 through m = 3 for the 150 V, 10 mg/s operating condition of the H6. The thruster is in an extremely strong global mode at $\boldsymbol{B_r/B_r^* = 0.52}$ (left), while some azimuthal perturbations visually appear at the nominal condition $\boldsymbol{B_r/B_r^* = 1}$ (middle), and stronger azimuthal perturbations still dominated by the global oscillation at $\boldsymbol{B_r/B_r^* = 1.48}$ (right).

The measured ion velocity distribution at the exit plane (z = 0 mm) for the low field magnitude condition of $B_r/B_r^* = 0.52$ (I_{IM} = 1.8 A) is plotted in Figure 8. The oscillation is similar to that observed at the nominal field, but there are a few notable differences in the VDF. The time-averaged distribution in this condition is by far the broadest found in this campaign, approximately spanning from 0 km/s to 12 km/s. The instantaneous velocity distribution is much narrower, an average of about 4 km/s. An ion population first forms near 3 km/s and then steadily increases in mean velocity with an almost constant spread. The highest ion density occurs near the minimum of mean velocity and gently decreases until the maximum mean velocity. After the VDF reaches a maximum in mean velocity, the population suddenly vanishes entirely within the noise level until another pulse begins at low mean velocity. A similar result was reported by Diallo[14] et al. using a heterodyne TRLIF technique, lending credence to the results of both new techniques (See FIG. 4). This effect may only reflect a depletion of the metastable population probed by LIF, not the ion density itself vanishing periodically in this very strong breathing oscillation.

The ion VDF at the high field condition $B_r/B_r^* = 1.48$ (I_{IM} = 5.5 A) has completely different behavior. Figure 9 shows that the population density remains steady at all times and the mean velocity oscillates chaotically within only a small range of about 1 km/s between 7 km/s and 8 km/s. The VDF FWHM is nearly constant at about 2 km/s.

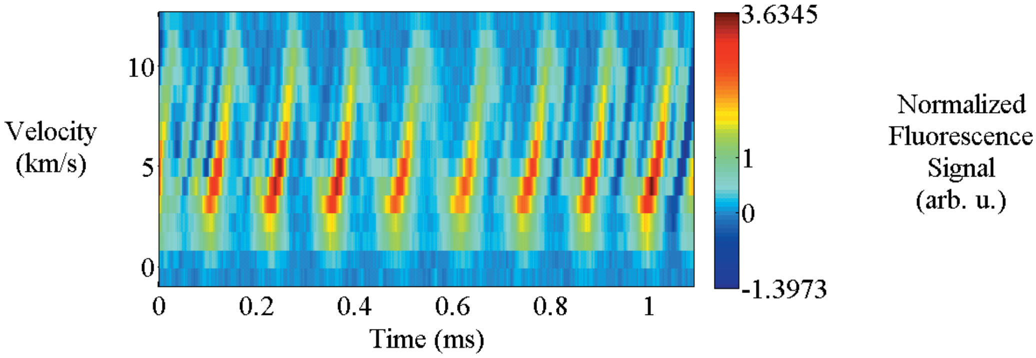

Figure 8. Ion velocity distribution as a function of time at z = 0 mm for the 150 V, 10 mg/s operating condition of the H6 with $B_r/B_r^* = 0.52$. Note that the metastable ion population probed appears to collapse entirely after the distribution reaches a maximum in mean velocity.

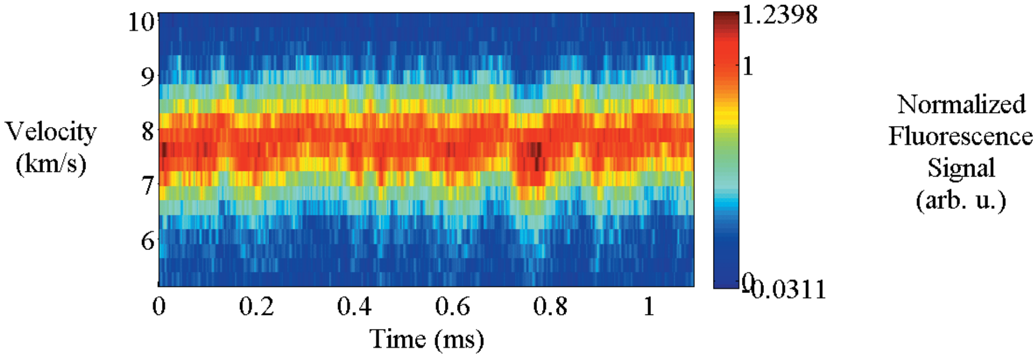

Figure 9. Ion velocity distribution as a function of time at z = 0 mm for the 150 V, 10 mg/s operating condition of the H6 with $B_r/B_r^* = 1.48$. The mean velocity oscillates less periodically and within a smaller range than it does at the lower field conditions.

C. Validation

TFLIF is a new technique never before applied to Hall thrusters, thus benchmarking is important to help assure that the results are accurate. The TFLIF system was first validated with a hollow cathode test bed using two types of controlled discharge current oscillations: periodic oscillations (reference 1) and a sinusoidal oscillation with randomly varying period (currently unpublished). The validation scheme involves a series of benchmark tests to confirm that TFLIF results agree with another measurement or theoretical prediction.

The first test is to compare the time-averaged ion VDF from TFLIF with the traditional time-averaged ion VDF measured with a lock-in amplifier. An example of this comparison is shown for the high field case ($B_r/B_r^* = 1.48$) in Figure 10. The average profile from TFLIF agrees with the lock-in amplifier profile within the noise of the lock-in amplifier measurement, which is roughly apparent because there are many closely spaced points with almost zero signal near the edge of the profile. In addition, the TFLIF profile is virtually identical to the triggered average LIF profile, with a mean absolute residual (the average of the absolute value of the difference between the two TRLIF measurements) of 0.16% of the peak value. These results are good evidence that TFLIF is not introducing systematic error, at least in the average LIF profile.

All other points presented in this paper have similar results, but the worst agreement was found at the low field condition, shown in Figure 11. The profiles do qualitatively agree, but it is not clear that the difference is within the noise of the lock-in amplifier. The issue stems both from poor velocity resolution in the lock-in amplifier profile and from laser tuning issues while acquiring that point. The laser had problems operating in a single mode at that time, and therefore the LIF profiles may not be entirely accurate due to mode completion and power fluctuations. The qualitative shape shared by all profiles is likely approximately accurate nonetheless.

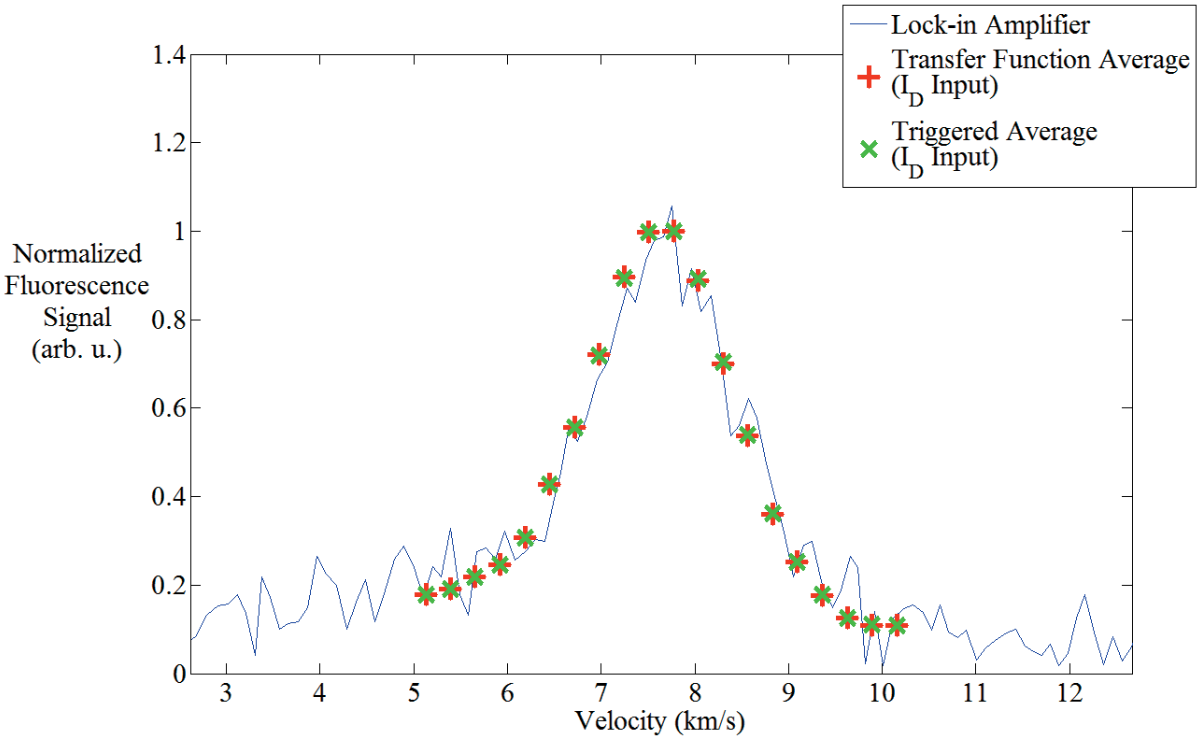

Figure 10. **A comparison showing the time-averaged ion VDF from TFLIF agrees with a traditional lock-in amplifier measurement of the time-averaged VDF. This example is for the z = 0 mm, $B_r/B_r^* = 1.48$ data set.**

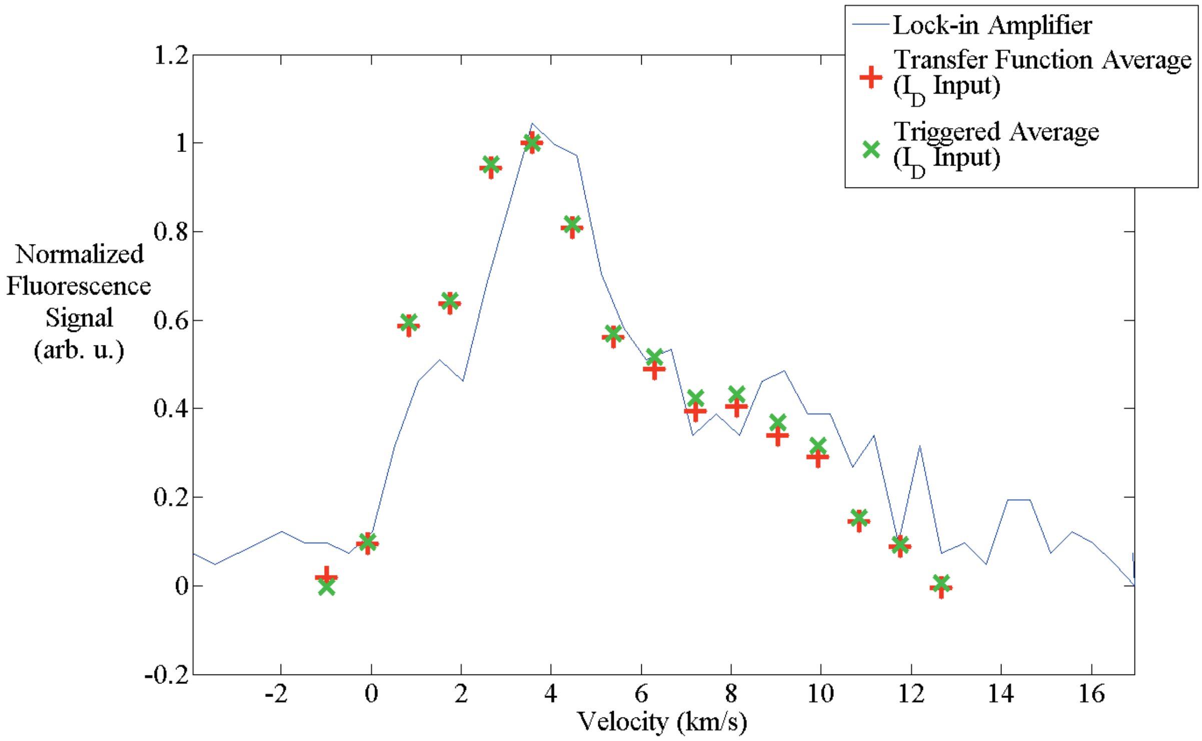

Figure 11. **A comparison of time-averaged LIF profiles for the z = 0 mm, $B_r/B_r^* = 0.52$ dataset. This dataset gave the worst agreement of the points in this paper, but the time-averaged ion VDF from TFLIF still**

generally agrees with a traditional lock-in amplifier measurement of the time-averaged VDF. The relatively poorer agreement is likely due to trouble with laser tuning while acquiring this point.

Even if the time-averaged profile from TFLIF is accurate, the time-resolved features could be distorted, so further benchmarks are necessary. A second test that is useful for periodic oscillations is to compare time-resolved TFLIF signal with the triggered average LIF signal. The triggered average uses the same filtering and phase-sensitive detection to condition the signal, but the transfer function average is replaced with the triggered average following phase-sensitive detection. The triggered average is the elementwise average of many time-series triggered at the same phase of the oscillation. This is equivalent to the averaging mode of many oscilloscopes. The two analysis techniques will theoretically converge to the same result if the system is linear and the oscillation is periodic. They converge because in that case the assumptions of both techniques are satisfied and they converge to the exact TRLIF signal[1]. This was demonstrated with a sinusoidal hollow cathode oscillation (not shown here) but in general is not possible with unperturbed Hall thruster oscillations since oscillations are not normally periodic.

The triggered average does not converge to the exact TRLIF signal in the case of nonperiodic oscillations. It typically exhibits an unphysical decay in the oscillation amplitude as the many time-series in the average are in phase at t = 0 but drift further out of phase from each other as time goes on. The oscillation is so nonperiodic for the $B_r/B_r^* = 1.48$ data set that the triggered average barely has an oscillation at all, as shown in Figure 12, and there are clear systematic differences with the TFLIF signal.

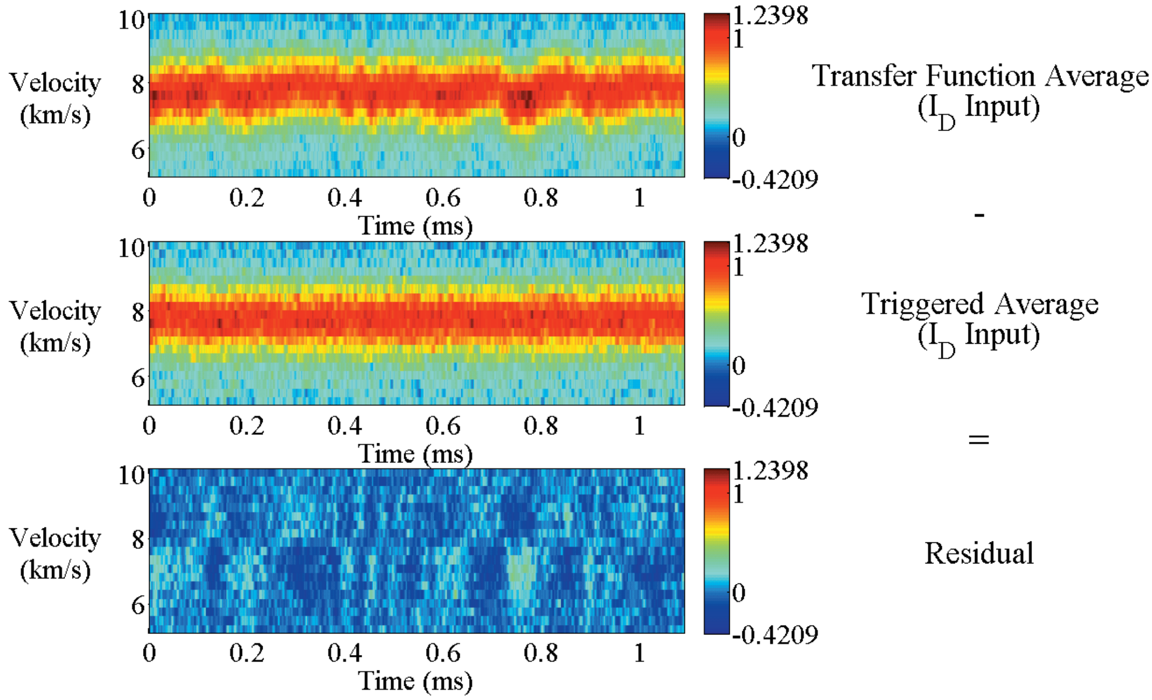

Figure 12. A direct comparison between the TFLIF signal and the triggered average LIF signal for the z = 0 mm, $B_r/B_r^* = 1.48$ data set shows major systematic differences. The triggered average shows a chaotic oscillation in the mean velocity but the triggered average fails to detect nonperiodic oscillations, hence another benchmark is required for nonperiodic oscillations.

It can be shown, however, that the transfer function's characteristic LIF output signal theoretically converges to the triggered average LIF signal if the triggered average discharge current is used as the input signal to the transfer function. This fact provides a general-purpose benchmark that can be used for all signals, periodic or not. An example of this comparison is shown in Figure 13, which shows that the average transfer function makes an excellent reproduction of the triggered average signal with only random noise and no systematic differences in the residual. This helps confirm that the assumptions that the transfer function analysis is based on are valid (e.g. that the system is linear, that reasonable analysis parameters were used, and that the average transfer function has sufficiently converged to the exact transfer function to give accurate results). If those assumptions were invalid, then we would expect some artifacts to be present in the transfer function's reproduction of the triggered average signal, leading to systematic differences in between it and the triggered average result.

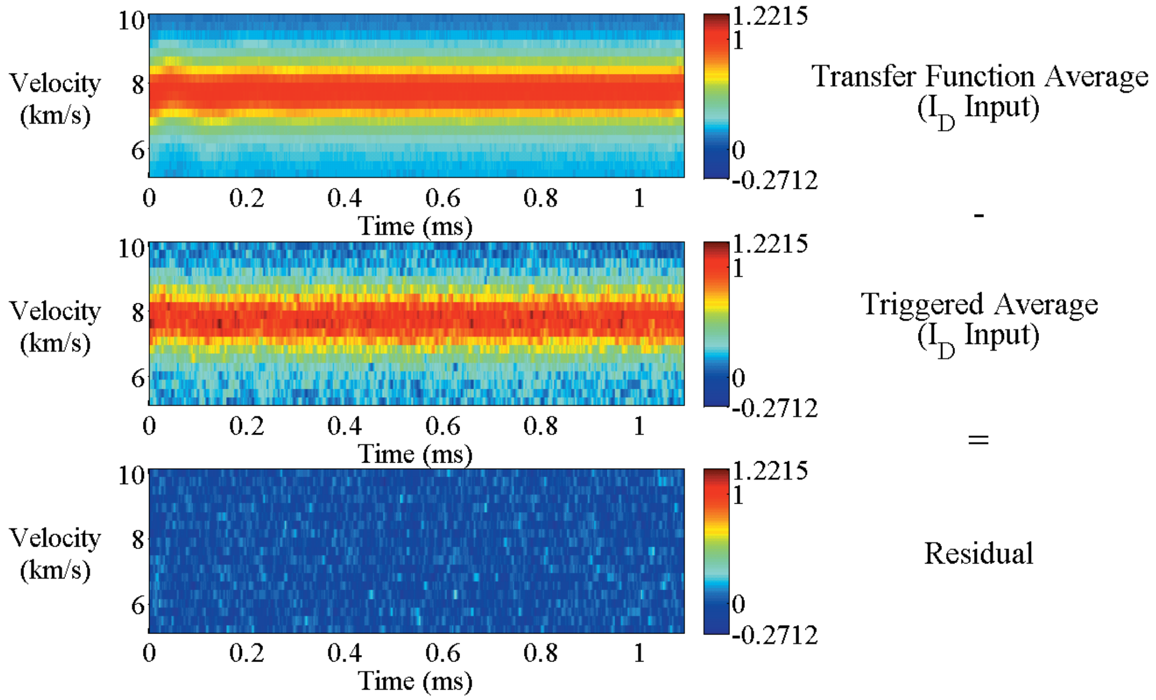

Figure 13. An example of the general-purpose benchmark with the z = 0 mm, $B_r/B_r^* = 1.48$ data set. The transfer function faithfully reproduces the triggered average LIF signal when the triggered average discharge current is used as input to the transfer function.

V. Conclusion

Major changes in ion dynamics were detected during a sweep of magnetic field magnitude from near the saturation limit of the magnetic circuit to near the minimum field with a stable discharge. We suspect that these changes in ion dynamics are related to a mode transition similar to the transitions previously observed by Brown[3] and Sekerak[4], but we are unable to make clear conclusions for a variety of reasons. The main reason is that time only allowed for LIF data at three magnetic field settings and three spatial locations. In addition, the transition observed may be fundamentally different than those previously observed by Brown and Sekerak with the H6. Unlike Brown's and Sekerak's transitions, the mean discharge current was approximately constant throughout the transition, and coherent spokes were not observed by the high-speed camera regardless of the magnetic field setting.

The evolution of the ion VDF was analyzed from a point 4 mm upstream of the exit plane to a point 15 mm downstream of the exit. It was found that the distribution width narrows downstream but oscillates between values approximately commensurate with velocity bunching predictions and values a few times the predicted width. A larger dataset is needed to make conclusions, but a distribution width wider than predicted by velocity bunching could be the result of processes such as ionization between the two points or collisions.

Overall, the importance of this campaign is to demonstrate time-resolved LIF signal recovery in a Hall thruster using the TFLIF technique. This campaign represents first TRLIF measurements on the H6 Hall thruster and, to our knowledge, the first TRLIF measurements on unperturbed Hall thruster operating conditions at a variety of magnetic field settings. The initial dataset shows interesting ion dynamics that call for more work to be done and will guide future LIF studies on the H6.

The problem with much lower SNR than previously reported at 150 V and 300 V discharge voltages with the H6 at this facility will be investigated in future work. With the SNR and facility issues resolved, we will conduct a more complete campaign at the nominal 300 V operating condition. It will be possible to measure TRLIF with a more dense spatial grid and magnetic field sweep. A more complete data set will allow us to better diagnose oscillations and mode transitions, and to estimate the time-varying electric field from the evolution of the ion velocity distribution.

Acknowledgments

The authors would like to thank Timothy B. Smith for discussion and helpful suggestions about the experimental setup.

This work was supported by AFOSR and AFRL through the MACEEP center of excellence Grant No. FA9550-09-1-0695.The authors would like to thank Dr. Mitat Birkan and Dr. Daniel Brown, the MACEEP program managers from AFOSR and AFRL, respectively.

References

[1] Durot, C. J., Gallimore, A. D., and Smith, T. B., "Validation and evaluation of a novel time-resolved laser-induced fluorescence technique," *Review of Scientific Instruments*, vol. 85, 2014, p. 013508.

[2] Huang, W., Drenkow, B., and Gallimore, A. D., "Laser-Induced Fluorescence of Singly-Charged Xenon inside a 6-kW Hall Thruster," *45th AIAA/ASME/SAE/ASEE Joint Propulsion Conference & Exhibit*, Denver, Colorado: 2009.

[3] Brown, D. L., and Gallimore, A. D., "Investigation of low discharge voltage hall thruster operating modes and ionization processes," *31st International Electric Propulsion Conference*, Ann Arbor, Michigan: 2009.

[4] Sekerak, M. J., Hofer, R. R., Polk, J. E., Longmier, B. W., Gallimore, A., and Brown, D. L., "Mode Transitions in Hall Effect Thrusters," *49th AIAA/ASME/SAE/ASEE Joint Propulsion Conference*, San Jose, CA: 2013.

[5] McDonald, M. S., and Gallimore, A. D., "Parametric Investigation of the Rotating Spoke Instability in Hall Thrusters," Wiesbaden, Germany: 2011.

[6] Scime, E., Biloiu, C., Compton, C., Doss, F., Venture, D., Heard, J., Choueiri, E., and Spektor, R., "Laser induced fluorescence in a pulsed argon plasma," *Review of scientific instruments*, vol. 76, 2005, p. 026107.

[7] Biloiu, C., Sun, X., Choueiri, E., Doss, F., Scime, E., Heard, J., Spektor, R., and Ventura, D., "Evolution of the parallel and perpendicular ion velocity distribution functions in pulsed helicon plasma sources obtained by time resolved laser induced fluorescence," *Plasma Sources Science and Technology*, vol. 14, Nov. 2005, pp. 766–776.

[8] Biloiu, I. A., Sun, X., and Scime, E. E., "High time resolution laser induced fluorescence in pulsed argon plasma," *Review of Scientific Instruments*, vol. 77, 2006, p. 10F301.

[9] MacDonald, N. A., Cappelli, M. A., and Hargus, W. A., "Time-synchronized continuous wave laser-induced fluorescence on an oscillatory xenon discharge," *Review of Scientific Instruments*, vol. 83, 2012, p. 113506.

[10] Mazouffre, S., Gawron, D., and Sadeghi, N., "A time-resolved laser induced fluorescence study on the ion velocity distribution function in a Hall thruster after a fast current disruption," *Physics of Plasmas*, vol. 16, 2009, p. 043504.

[11] Mazouffre, S., and Bourgeois, G., "Spatio-temporal characteristics of ion velocity in a Hall thruster discharge," *Plasma Sources Science and Technology*, vol. 19, Dec. 2010, p. 065018.

[12] Bourgeois, G., Mazouffre, S., and Sadeghi, N., "Examination of the temporal characteristics of the electric field in a Hall effet thruster using a photon-counting technique," *31st International Electric Propulsion Conference, Ann Arbor, MI*, 2009.

[13] Vaudolon, J., Balika, L., and Mazouffre, S., "Photon counting technique applied to time-resolved laser-induced fluorescence measurements on a stabilized discharge," *Review of Scientific Instruments*, vol. 84, 2013, p. 073512.

[14] Diallo, A., Keller, S., Shi, Y., Raitses, Y., and Mazouffre, S., "Time-resolved ion velocity distribution in a cylindrical Hall thruster: Heterodyne-based experiment and modeling," *Review of Scientific Instruments*, vol. 86, Mar. 2015, p. 033506.

[15] Lobbia, R. B., and Gallimore, A. D., "A method of measuring transient plume properties," *AIAA Paper*, vol. 4650, 2008, p. 2008.

[16] Huang, W., Reid, B. M., Smith, T. B., and Gallimore, A. D., "Laser-Induced Fluorescence of Singly-Charged Xenon in a 6kW Hall Thruster," Hartford, CT: 2008.

[17] Reid, B. M., "The influence of neutral flow rate in the operation of Hall thrusters," Ph.D. dissertation, University Of Michigan, 2009.

[18] Kaufman, S. ., "HIGH-RESOLUTION LASER SPECTROSCOPY IN FAST BEAMS," *Optics Communications*, vol. 17, Jun. 1976, pp. 309–312.

[19] Field, D., and Gray, M. D., "Kinematic compression and expansion of the velocity distributions of particles in gas flows," *Physical Review A*, vol. 40, 1989, p. 1976.